Improving Wireless Communications Using Multiple Antennas

Miguel Bazdresch
ECTET Dept.
Rochester Institute of Technology
Rochester, New York
email: mxbiee@rit.edu

Joaquin Cortez
Electrical Engineering Dept.
ITSON University
Cd. Obregon, Mexico
email: jcortez@itson.mx

***Abstract*—Space-time coding and multiple-input, multiple-output wireless system promise to deliver higher data rates with higher reliability than traditional systems, with no increase on transmit power or bandwidth. In this expository paper, we present multiple-antenna systems and their ability to increase the number of dimensions that may be transmitted per channel use. We present two space-time codes, one that is oriented towards maximizing the data rate (V-BLAST) and the other towards increasing reliability (Alamouti). We present a third option, a hybrid code, that has the advantages of both types of coding. This code belongs to the general class of linear dispersion codes, and it has a particular structure that allows the design of a hardware receiver with very low complexity.**

***Index Terms*—DSTTD, Hybrid Space-Time Codes, Givens rotations, CORDIC algorithm, Sorted QR Decomposition.**

I. Introduction

Consider the problem of transmitting a sequence of real numbers $S = s_1, s_2, \ldots, s_n$, where the sequence consists of n numbers taken from the set $\mathcal{Q} = \{q_1, q_2, \ldots, q_k\}$, over an electronic communications channel. This can be accomplished by selecting a set of functions $\mathcal{F} = \{f_1, f_2, \ldots, f_n\}$ such that

$$\int_{-\infty}^{\infty} f_i(t) f_j(t) dt = 0 \tag{1}$$

whenever $i \neq j$, where i and j take values between 1 and n, and also

$$\int_{-\infty}^{\infty} f_i(t) f_i(t) dt = 1. \tag{2}$$

A set $\mathcal{F}$ that meets these two conditions is called an orthonormal set of functions. The sequence S may then be transmitted by forming the signal

$$x(t) = \sum_i s_i f_i(t). \tag{3}$$

The orthonormality of the signals in $\mathcal{F}$ allows the receiver to recover the transmitted numbers using

$$s_i = \int_{-\infty}^{\infty} x(t) f_i(t) dt. \tag{4}$$

This method is illustrated in Figure 1.

In the presence of a random, white noise signal $v(t)$, then the received signal is $r(t) = x(t) + v(t)$ and the numbers cannot be recovered without error. The receiver may estimate each number as

$$\begin{aligned} \hat{s_i} &= \int_{-\infty}^{\infty} r(t) f_i(t) dt \qquad (5)\\ &= s_1 + v, \qquad (6) \end{aligned}$$

where v is a Gaussian random variable with zero mean and variance equal to $N_0/2$. As long as the numbers q_i are sufficiently separated and the noise variance is low enough, then reliable communication is possible by applying the following rule in the receiver: having received $\hat{s_i}$, estimate the transmitted number as the element of $\mathcal{Q}$ that is closer to $\hat{s_i}$ using Euclidean distance.

In most cases, the sequence of numbers to transmit is very large. Finding a corresponding set of orthonormal functions may seem like a hard problem, but in fact it is not. It has been proved that, given a time interval of duration T, and an available bandwidth B, then a set of orthonormal signals $\mathcal{F}$ of duraton T and bandwidth B with $2BT$ elements exists. The importance of this results is that it imposes a limit on the rate at which transmission may be accomplished; that is, at most 2 numbers may be transmitted, per available hertz of bandwidth, per second.

An interesting and very useful analogy may be made between orthonormal vectors and orthonormal signals. Just as a set of n vectors define the axes of an Euclidean space of n dimensions, the set $\mathcal{F}$ of n orthonormal signals also define an Euclidean space of the same number of dimensions. The sequence S becomes a vector $\mathbf{S}$, where each element s_i defines the coordinate of the vector along the direction of f_i. We say, then, that it is possible to transmit 2 dimensions per available hertz per second. Note that, if the numbers that are transmitted are complex, then we say we may transmit one complex dimension per hertz per second.

This theoretical limit on transmission seems insurmountable. However, it is based on the initial assumption that the channel reproduces at the receiver end a voltage produced at the transmitter end. This assumption is not true for the wireless channel. In this channel, the signal received by an antenna is the sum of all signals transmitted by all antennas that are within its range. Furthermore, each transmited signal is subject to different channel conditions that result in different amounts of fading, delay, interference, attenuation and noise. The question is then, what is the number of dimensions that may be transmitted on this channel? And, what tranmsission schemes may be required to take advantage of those extra dimensions, if any?

Consider a wireless transmitter with n_T antennas. Each antenna transmits independently of the others, but all use the same bandwidth and all share the available transmit power. The elements of S are transmitted n_T at a time. At the receiver, there are n_R antennas, all receiving signals over the same bandwidth. The wireless channel presents slow fading, which means that each transmitted signal experiences an attenuation and a delay. The attenuation and delay are different and independent for each pair of transmit and receive antennas. This system may be modeled as

$$\mathbf{r} = \mathbf{H}\mathbf{s} + \mathbf{v}, \tag{7}$$

s is the transmitted signal vector, consisting of n_T complex numbers. **H** is a complex matrix of size $n_R \times n_T$; element h_{ij} is the channel gain between transmit antenna j and receive antenna i, and is a random Gaussian variable of zero mean and variance 1/2 per dimension. Vector **v** is the noise vector; its n_R elements are random Gaussian variables of zero mean and variance $N_0/2$. Finally, each of the n_R elements of vector **r** signal received by one of the receiver antennas. This kind of system is known as a multiple-input, multiple-output (MIMO) wireless system, and it is illustrated in Figure 2.

Now we focus on the effect of matrix **H** on the information vector **s**. A matrix rotates and scales vectors. This is illustrated in Figure 3. What is most important is that the matrix changes the coordinates of the vector, which may result in compression of the vector in one or more dimensions. When this happens, then the separation between the received vector elements becomes smaller and the system becomes more susceptible to noise.

In spite of these apparent difficulties, it can be shown that the wireless channel does increase the number of dimensions in the communications system. This can be seen with help from the matrix singular value decomposition. Any matrix **H** may be expressed as the product of three matrices:

$$\mathbf{H} = \mathbf{U}\mathbf{S}\mathbf{V}^*. \tag{8}$$

(Here, $\mathbf{V}^*$ means the complex conjugate of **V**). Matrices **U** and **V** are orthogonal, while matrix **S** is diagonal. This means that $\mathbf{H}\mathbf{x} = \mathbf{U}\mathbf{S}\mathbf{V}^*$ takes vector **x**, rotates it, then scales it, then rotates it again. In theory, then, the transmitter could pre-rotate the vector to be sent, and the receiver could post-rotate it, to counteract the effects of the channel matrix. More precisely: in order to transmit vector **x**, the transmitter calculates and sends vector $\mathbf{V}^*\mathbf{x}$. The channel will scale it and rotate it, so the received vector will be:

$$\mathbf{r}' = \mathbf{H}\mathbf{V}^*\mathbf{x} = \mathbf{U}\mathbf{S}\mathbf{x}. \tag{9}$$

The receiver undoes the larst rotation:

$$\mathbf{r} = \mathbf{U}^*\mathbf{r}' = \mathbf{S}\mathbf{x}. \tag{10}$$

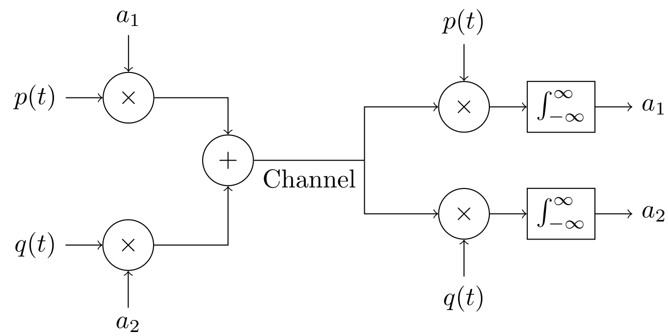

Fig. 1: Transmission of two numbers, a_1 and a_2, using orthonormal signals $p(t)$ and $q(t)$. The channel is an electronic medium. In the absence of noise, the numbers are recovered perfectly by the receiver.

So, the multiple-antenna wireless channel has the effect of scaling each dimension of the transmit vector by the singular values of the channel matrix. In effect, this means that the channel may transmit $2n_T$ dimensions per second per hertz. This is illustrated in Figure 4.

The SVD formulation is useful to prove the potential of the wireless channel, but not necessarily to effectively make use of it. The reason is that calculating the SVD is computationally expensive, and also because the transmitter needs to have knowledge of **V**, which is usually to available.Space-time codes are a set of transmission and reception schemes that attempt to make use of the extra dimensions afforded by the wireless channel to improve data rate, reliability, or both. The following sections explore three different space-time codes and their performance. In Section II, we present three space-times codes in more detail. In Section III we introduce the correlated wireless channel, which presents significant obstacles to wireless communications. In Section IV, we introduce a hybrid code with two particular properties: first, it is a linear dispersion code, which means that it may be epxresses as a spatial multiplexing code; second, its particular structure allows the design of a low complexity hardware receiver, which is also described in detail. In Section V we present simulation results that show the performance of each code when configured to have identical data rates. Finally, we present our conclusions in Sectin VI.

II. Space-Time Codes

A MIMO system employs multiple antennas, both at the transmitter and the receiver, creating time and spatial diversity. Two general techniques have been devised to take advantage of MIMO systems: *Spatial Multiplexing* and *Diversity Transmission*. Spatial multiplexing relies on signal processing at the receiver to create multiple independent transmit channels, resulting in very high spectral efficiency with a simple coding scheme. One of the better known spatial multiplexing techniques is V-BLAST [5]. Diversity transmission, on the other hand, increases diversity gain, improving link reliability; this is achieved for instance by orthogonal Space-Time Block Codes

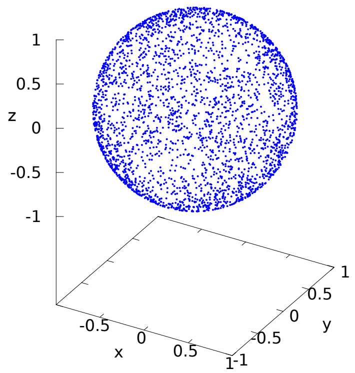

(a) Vectors on the surface of a 3-D sphere.

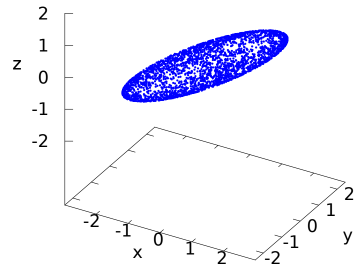

(b) The same vectors, multiplied by a random matrix.

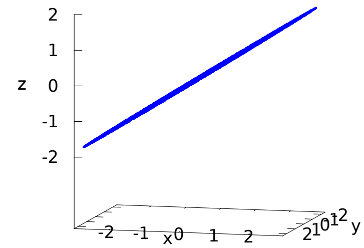

(c) A different perspective on the same vectors. It can be seen that multiplying by a matrix may compress some of the original dimensions; in this example, a sphere has been turned into an elongated disc.

Fig. 3: The effect of matrix multiplication on vectors, represented geometrically. A matrix multiplication scales, rotates, then scales again a vector. Here, the effect is illustrated on vectors on the surface of a sphere.

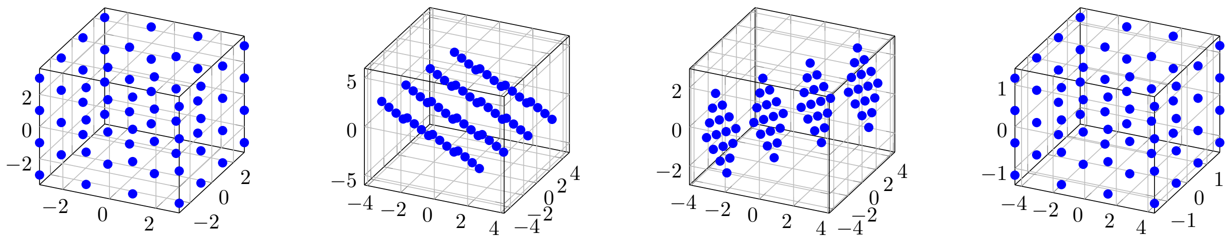

(a) (b) (c) (d)

Fig. 4: An illustration of the number of dimensions available in the wireless channel. In (a), each blue dot represents a 3-D signal. This set of signals is pre-rotated before transmission (b). The channel rotates and scales the signals (c), which are finally post-rotated at the receiver. This shows that the channel may transmit signals in three dimensions.

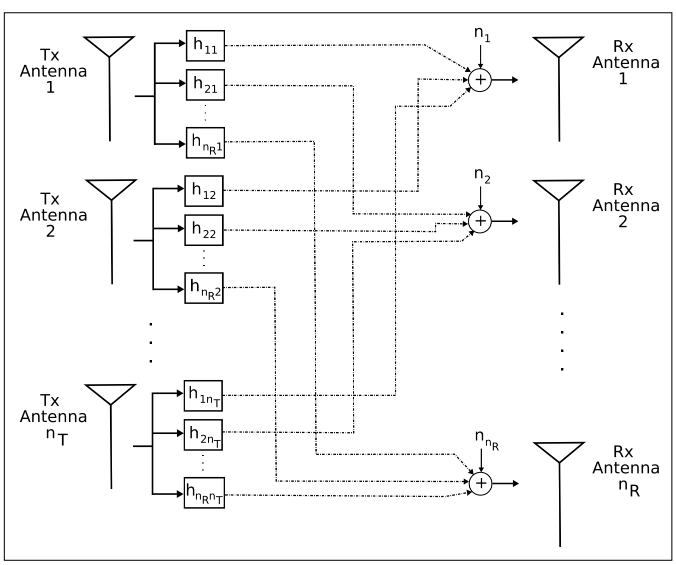

Fig. 2: A system with multiple transmit and receive antennas. The signal between each pair of antennas is multiplied by the channel gain, which changes the signal's amplitude and phase. Each antenna receives also a noise signal. All channel gains and noise signals are indepenent of each other.

(STBC). While their spectral efficiency is not as high as that of V-BLAST, they offer better bit-error rates (BER) and a simple maximum-likelihood decoding algorithm [15].

A. V-BLAST

A V-BLAST system consists of n_T transmit antennas operating at the same frequency band with synchronized symbol timing. All n_T antennas use the same signal constellation S, and each transmitted symbol has average energy E_s. The receiver consists of n_R antennas, where $n_R \geq n_T$. Such a system is often referred to as an (n_T, n_R) antenna array. The channel is modeled as a complex matrix $\mathbf{H}$ of size $n_R \times n_T$, where each element h_{ij} of $\mathbf{H}$ is the complex transfer function from transmitter j to receiver i. The channel is assumed to remain constant during the transmission of a block of L symbols, and then change in an independent fashion. A full description of the V-BLAST algorithm is given in [5].

B. Alamouti and DSTTD

An Alamouti space-time transmit diversity (STBC) [15] is a mapping of symbols to combinations of time intervals and antennas. This mapping may be represented by a table or a matrix, where each row corresponds to a transmit antenna and each column to a time interval. As an example, consider a system with $n_T = 2$; the vector to be transmitted is $\mathbf{s} = [s_1\ s_2]$. The STBC given by

$$\mathbf{S} = \begin{bmatrix} s_1 & -s_2^* \\ s_2 & s_1^* \end{bmatrix} \tag{11}$$

specifies that, at the first symbol interval, antenna 1 transmits s_1 and antenna 2 transmits s_2. During the second interval, antenna 1 transmits $-s_2^*$ and antenna 2 transmits s_1^*.

The double space-time transmit diversity (DSTTD) system was proposed as a simple way to obtain transmit diversity gain and spatial multiplexing gain simultaneously. It consists of two Alamouti space-time transmit diversity (STTD) units. Alamouti's STTD itself gives transmit diversity gain and its dual structure improves spatial multiplexing gain. In addition, it demands fewer receive antennas than transmit antennas, which may be beneficial in many practical applications.

C. Hybrid Codes

In general, the transmission process of a hybrid scheme can be divided in layers, like V-BLAST. However, in contrast to V-BLAST, in the hybrid case a layer may consist of a stream of symbols at the output of an STBC encoder (possibly Alamouti), which is transmitted by a group of antennas, or of an uncoded stream, which is transmitted from a single antenna. Based on this concept of layers, hybrid MIMO transceiver schemes combine pure diversity with pure spatial multiplexing schemes. With this idea, hybrid MIMO schemes achieve a compromise between spatial multiplexing and diversity transmission gains. The basic idea behind these structures is to combine array processing and space-time coding, as presented in [6].

III. Channel Correlation

The uncorrelated channel model has large capacity [1]; however, in many real propagation environments the fades among antennas are not independent. When this is caused by insufficient spacing of antennas and relative displacement between transmitter and receiver, the phenomenon is commonly called spatial selectivity (SS); it is said that the channel is under spatial correlation (SC) conditions. Under these conditions, channel capacity is significantly degraded [2]. The channel model becomes

$$\mathbf{H}_c = \left(R_H^{R_x}\right)^{\frac{1}{2}} \mathbf{H} \left(R_H^{T_x}\right)^{\frac{1}{2}}, \tag{12}$$

where $\mathbf{H}$ is the uncorrelated channel matrix, $R_H^{T_x}$ is the transmitted correlation matrix, and $R_H^{R_x}$ is the received correlation matrix (see [3], [4] and references therein).

The properties of the correlation matrices depend on the antenna array topology; here, we consider linear arrays only. Furthermore, signal power depends on the transmitter's signal angle of departure (φ^{Tx}) and the receiver's angle of arrival (φ^{Rx}). This information is summarized in the system's cross-Power Azimuth Spectrum $p(\varphi)$ (PAS), where φ is the array's

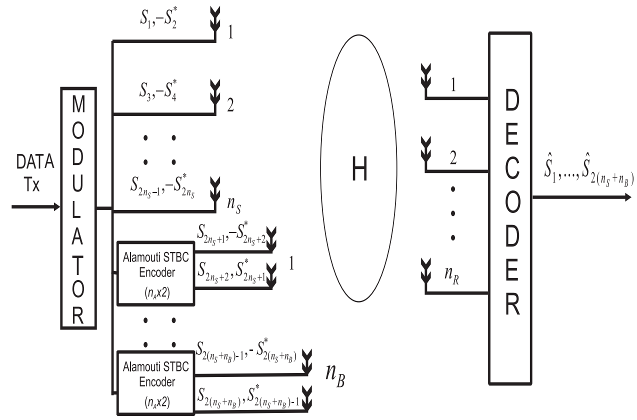

Fig. 5: Block diagram of the ZF LD STBC-VBLAST hybrid code. The code consists of n_S spatial layers and n_B diversity layers.

TABLE I: ZF LD STBC-VBLAST Symbol to Antenna Mapping with $k = B - 1 + n_S$

	Spatial Antennas S_{spa}	STBC Blocks S_A $B = 1, \cdots, n_B$	
Time	Antenna $V = 1, 2, \cdots, n_S$	Antenna 1	Antenna 2
t	s_V	s_{kn_A+1}	s_{kn_A+2}
$t+T$	$-s^*_{V+1}$	$-s^*_{kn_A+2}$	$s^*_{kn_A+1}$

azimuthal angle. In this paper, we will evaluate the performance of space-time codes under Laplacian PAS correlation, which is given by

$$p(\varphi) = \frac{e^{-\frac{1}{k}|\varphi|}}{2k\left(1 - e^{\frac{-\pi}{k}}\right)} \tag{13}$$

for $-\pi \leq \varphi \leq \pi$.

IV. A Hybrid Code: ZF LD STBC-VBLAST

In this section we present a hybrid code called ZF LD STBC-VBLAST. A simplified block diagram is shown in Figure 5. A single data stream is demultiplexed into n_L spatial layers, and each of them is mapped to the chosen constellation. Symbols are mapped to two different kinds of transmitters: n_S V-BLAST layers and n_B STBC encoders with $n_A = 2$ antennas each; therefore, $n_T = n_S + 2n_B$. It is assumed that $n_R \geq n_S + n_B$. In the transmission of one block, the symbol sequence is $s_1, s_2, \ldots, n_{sym} = s_{2(n_S+n_B)}$. The mapping of symbols to antennas is shown in Table I. The power allocated to the V-BLAST encoder is $P_S = 2/n_{sym}$, while the power allocated to the Alamouti encoder is $P_A = P_S/2$. This allocation results in all symbols being transmitted with the same energy, which is the optimal strategy in the absence of channel side information (CSI) at the transmitter.

A. Hybrid Code Receiver Architecture

Under the assumption that channel side information is perfectly known at the receiver, the received signal may be written as:

$$\begin{bmatrix} y_1^{(1)} \, y_1^{(2)} \\ \vdots \quad \vdots \\ y_{n_R}^{(1)} \, y_{n_R}^{(2)} \end{bmatrix} = \begin{bmatrix} h_{1,1} & \cdots & h_{1,n_T} \\ \vdots & \ddots & \vdots \\ h_{n_R,1} & \cdots & h_{n_R,n_T} \end{bmatrix} \begin{bmatrix} S_{spa} \\ S_A \end{bmatrix} + \begin{bmatrix} n_1^{(1)} \, n_1^{(2)} \\ \vdots \quad \vdots \\ n_{n_R}^{(1)} \, n_{n_R}^{(2)} \end{bmatrix} \tag{14}$$

or, in matrix notation,

$$Y = HS + N. \tag{15}$$

Reformulating the system equation (14) as a linear dispersion code [8], we have:

$$\begin{bmatrix} y_1^{(1)} \\ y_1^{(2)^*} \\ \vdots \\ y_{n_R}^{(1)} \\ y_{n_R}^{(2)^*} \end{bmatrix} = \begin{bmatrix} H_{spa} & H_A \end{bmatrix} S_{LD} + \begin{bmatrix} n_1^{(1)} \\ n_1^{(2)^*} \\ \vdots \\ n_{n_R}^{(1)} \\ n_{n_R}^{(2)^*} \end{bmatrix}. \tag{16}$$

The complete process of this transformation is explained in [14]. Equation (16) can be expressed in compact form as:

$$Y_{LD} = H_{LD} S_{LD} + N_{LD}, \tag{17}$$

where block matrix H_{LD} is a linear dispersion matrix. One block corresponds to the V-BLAST layers and the the other to the STBC layers. The V-BLAST block H_{spa} is given by:

$$H_{spa} = \begin{bmatrix} H_{1,1}^{spa} & \cdots & H_{1,n_S}^{spa} \\ \vdots & \ddots & \vdots \\ H_{n_R,1}^{spa} & \cdots & H_{n_R,n_S}^{spa} \end{bmatrix}, \tag{18}$$

where

$$H_{ij}^{spa} = \begin{bmatrix} h_{i,j} & 0 \\ 0 & -h_{i,j}^* \end{bmatrix}, \tag{19}$$

for $i = 1, 2, \cdots, n_R$ and $j = 1, 2, \cdots, n_S$. The STBC block H_A is itself a block matrix; it is given by:

$$H_A = \begin{bmatrix} H_{1,1}^A & \cdots & H_{1,n_B}^A \\ \vdots & \ddots & \vdots \\ H_{n_R,1}^A & \cdots & H_{n_R,n_B}^A \end{bmatrix}, \tag{20}$$

where each element of H_A is given by:

$$H_{kB}^A = \begin{bmatrix} h_{k,2B+n_S-1} & h_{k,2B+n_S} \\ h_{k,2B+n_S}^* & -h_{k,2B+n_S-1}^* \end{bmatrix}, \tag{21}$$

for $k = 1, 2, \ldots, n_R$ and $B = 1, 2, \ldots, n_B$. The matrix H_{ij}^{spa} is the portion of H_{LD} that links the j^{th} spatial antenna with the i^{th} receiver antenna. Likewise, H_{kB}^A links the B^{th} STBC block to the k^{th} receiver antenna.

The reformulation of equation (14) as equation (16) transforms the hybrid code into a simpler, equivalent, purely spatial system with $N_T = 2(n_S + n_B)$ transmit antennas and without distinction between the STBC and V-BLAST layers. This is illustrated in Figure 6.

By changing the number of layers and the modulation type, it is possible to arrange V-BLAST, DSTTD and hybrid schemes to have the same bandwidth efficiency. For instance, in Table II we show configurations that allow transmission of 12 bits per channel use.

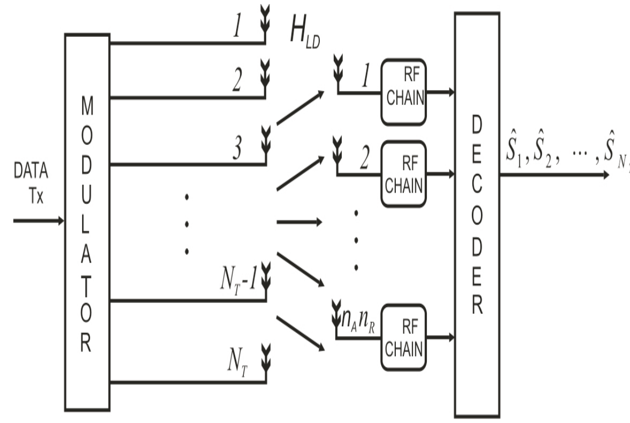

Fig. 6: A hybrid system equivalent to that of Figure 5, once it has been converted to a linear dispersion code. This conversion means that all known results for spatial-multiplexing codes are immediately applicable to this hybrid code.

TABLE II: Three space-time coding configurations with the same spectral efficiency: 12 bits per channel use.

Scheme	n_S	n_B	Modulation
VBLAST	4	0	8-PSK
Hybrid	2	1	16-QAM
DSTTD	0	2	64-QAM

B. OSIC detection for hybrid codes

In the three configurations proposed above, we can used tne same *HC Sorted QR Decomposition* detector. We first find $H_{LD} = Q_{LD} R_{LD}$, where Q_{LD} is unitary and R_{LD} is upper triangular. By multiplying the received signal Y_{LD} by Q_{LD}^H, we obtain a new receive vector given by $\tilde{Y}_{LD} = R_{LD} S_{LD} + \tilde{N}_{LD}$, which is fully equivalent, but can be solved with significantly reduced computational complexity through back-substitution. The decoding steps are presented in Figure 7.

Matrix H_{LD} is $2n_R \times N_T$. A direct application of Givens rotations to calculate its *HC Sorted QR* Decomposition would result in unacceptable complexity. However, we use the CORDIC algorithm [18] to calculate the QR matrix decomposition, as follows. A CORDIC block is a circuit that performs the following iteration on its two inputs, X and Y:

$$X_{i+1} = X_i - m\sigma 2^{-i} Y_i \tag{22}$$

$$Y_{i+1} = Y_i + \sigma 2^{-i} X_i, \tag{23}$$

where $\sigma = -sign(Y)sign(X)$. Parameter m is provided by a control unit. If $m = 0$ then the block is said to be operating in vectoring mode, if $m = 1$ then it is on rotational mode. After a number of steps, the iteration converges to the desired result. A diagram of a CORDIC block is shown in Figure 8.

We define the notation used to indicate the two operations required to perform Givens rotations using the CORDIC algorithm. We assume that $Z = a + jb$ denotes a complex number:

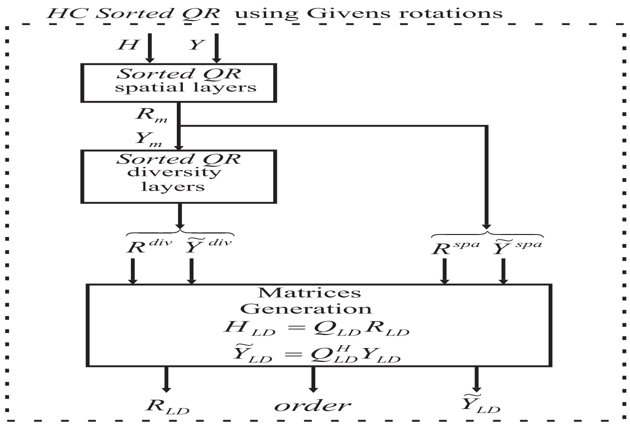

Fig. 7: Detection process for hybrid codes. Using Givens rotations, this process may be implemented in hardware with low complexity.

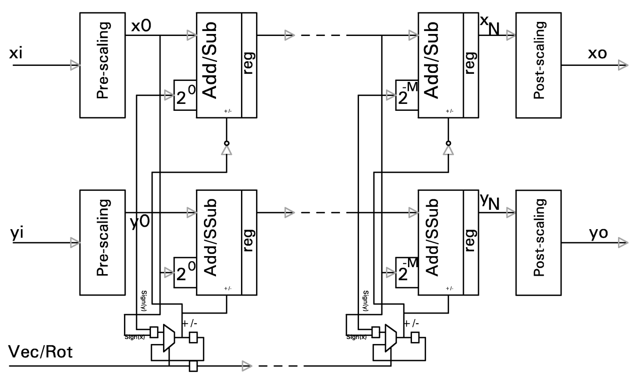

Fig. 8: Diagram of a CORDIC processor.

- **Vectoring Mode**. The vectorial operation of the CORDIC is denoted as $[X_r\ \theta] = \mathbf{V}(a, b)$.
- **Rotational Mode**. The rotation operation of the CORDIC is denoted as $[X_r\ X_i] = \mathbf{R}(a, b, \theta)$.

To reduce the complexity, we propose to obtain the QR decomposition of the H_{LD} matrix in two stages: first we obtain the QR decomposition corresponding to the *spatial layers* of the hybrid system; in the second stage we calculate the QR decomposition for the *diversity layers*. As a first step, we calculate the Sorted QR decomposition of matrix H_m, defined as:

$$H_m = \begin{bmatrix} h_{1,1} & h_{1,2} & \cdots & h_{1,n_T} & y_{1,1} & y_{1,2} \\ \vdots & \vdots & \ddots & \vdots & \vdots & \vdots \\ h_{n_R,1} & h_{n_R,2} & \cdots & h_{n_R,n_T} & y_{n_R,1} & y_{n_R,2} \end{bmatrix}. \tag{24}$$

We apply a series of orthogonal transformations Θ using Givens rotations over matrix H_m to obtain matrix $\overline{H}_m$:

$$\overline{H}_m = \begin{bmatrix} r_{1,1} & r_{1,2} \cdots & r_{1,n_S} & r_{1,k} & \cdots & r_{1,n_T} & \tilde{y}_{1,1} & \tilde{y}_{1,2} \\ 0 & r_{2,2} \cdots & r_{2,n_S} & r_{2,k} & \cdots & r_{2,n_T} & \tilde{y}_{2,1} & \tilde{y}_{2,2} \\ \vdots & \vdots \ddots & \vdots & \vdots & \vdots & \vdots & \vdots & \vdots \\ 0 & 0 \cdots & r_{n_S,n_S} & r_{n_S,k} & \cdots & r_{n_S,n_T} & \tilde{y}_{n_S,1} & \tilde{y}_{n_S,2} \\ 0 & 0 \cdots & 0 & \overline{h}_{k,k} & \cdots & \overline{h}_{k,n_T} & \overline{y}_{k,1} & \overline{y}_{k,2} \\ 0 & 0 \cdots & 0 & \overline{h}_{k+1,k} & \cdots & \overline{h}_{k+1,n_T} & \overline{y}_{k+1,1} & \overline{y}_{k+1,2} \\ \vdots & \vdots \ddots & \vdots & \vdots & \ddots & \vdots & \vdots & \vdots \\ 0 & 0 \cdots & 0 & \overline{h}_{n_R,k} & \cdots & \overline{h}_{n_R,n_T} & \overline{y}_{n_R,1} & \overline{y}_{n_R,2} \end{bmatrix}, \tag{25}$$

where $k = n_S + 1$. In this process, we also produce vector *order* which specifies the detection order of the spatial layers. The process applied in this stage is shown as Algorithm (1).

Algorithm 1 Spatial Decomposition of *HC Sorted QR* using Givens Rotations

INPUT: $H_m^{n_R \times n_T + L}$, L, N_T, n_S.
OUTPUT: $\overline{H}_m$ and *order*
$\overline{H}_m = H_m$, $order = [1:1:N_T]$.
for $i = 1$ to n_S **do**
  $k = \operatorname{argmin}_{j=i:n_S} \|(\overline{H}_m(:,j))\|_2$
  exchange columns i and k of $\overline{H}_m$.
  exchange columns $Li:-1:Li-(L-1)$ and $Lk:-1:Lk-(k-1)$ of vector *order*
  for $l = i+1$ to n_R **do**
    for $m = n_T+2:2$ to n_T+L **do**
      $\overline{H}_m(l,m) = -\overline{H}_m(1,m)^*$
    end for
  end for
  for $l = i$ to n_R **do**
    $[x_r\ \theta] = \mathbf{V}\big(\mathbf{Re}(\overline{H}_m(l,i)), \mathbf{Im}(\overline{H}_m(l,i))\big)$
    $\overline{H}_m(l,i) = x_r + j*0$
    for $m = i+1$ to n_T+L **do**
      $[x_r\ x_i] = \mathbf{R}\big(\mathbf{Re}(\overline{H}_m(l,m)), \mathbf{Im}(\overline{H}_m(l,m)), \theta\big)$
      $\overline{H}_m(l,m) = x_r + j*x_i$
    end for
  end for
  for $l = i+1$ to n_R **do**
    for $m = n_T+2:2$ to n_T+L **do**
      $\overline{H}_m(l,m) = -\overline{H}_m(1,m)^*$
    end for
  end for
  for $l = n_R:-1$ to $i+1$ **do**
    $[x_r\ \phi] = \mathbf{V}\big(\mathbf{Re}(\overline{H}_m(l-1,i)), \mathbf{Re}(\overline{H}_m(l-1,i))\big)$
    $\overline{H}_m(l-1,i) = x_r + j*0$
    $\overline{H}_m(l,i) = 0 + j*0$
    for $m = i+1$ to n_T+L **do**
      $[x_1\ x_2] = \mathbf{R}\big(\mathbf{Re}(\overline{H}_m(l-1,m)), \mathbf{Re}(\overline{H}_m(l,m)), \phi\big)$
      $[x_3\ x_4] = \mathbf{R}\big(\mathbf{Im}(\overline{H}_m(l-1,m)), \mathbf{Im}(\overline{H}_m(l,m)), \phi\big)$
      $\overline{H}_m(l-1,m) = x_{r1} + j*x_{i1}$
      $\overline{H}_m(l,m) = x_{r2} + j*x_{i2}$
    end for
  end for
end for

Then, we select the first n_S rows of $\overline{H}_m$ to build the matrices R^{spa} and $\tilde{Y}^{spa}$, which have the following form:

$$R^{spa} = \begin{bmatrix} r_{1,1} \, r_{1,2} \cdots \; r_{1,n_T} \\ 0 \;\; r_{2,2} \cdots \; r_{2,n_T} \\ \vdots \;\;\; \vdots \;\; \ddots \;\;\; \vdots \\ 0 \;\;\; 0 \;\; \cdots r_{n_S,n_T} \end{bmatrix}, \tag{26}$$

$$\tilde{Y}^{spa} = \begin{bmatrix} \tilde{y}_{1,1} & \tilde{y}_{1,2} \\ \vdots & \vdots \\ \tilde{y}_{n_S,1} & \tilde{y}_{n_S,2} \end{bmatrix}. \tag{27}$$

The matrices R^{spa} and $\tilde{Y}^{spa}$ represent the contribution of the spatial layers in the hybrid scheme.

In the second stage of the QR decomposition, dedicated to the diversity layers, the non-normalized elements $\overline{h}_{i,j}$ in equation (25) are used to build the matrix H^{ala}_{div}, which has the following structure (assuming $k = n_S + 1$):

$$H^{ala}_{div} =$$

$$\begin{bmatrix} \overline{h}_{k,k} & \overline{h}^*_{k,k+1} & \cdots & \overline{h}_{k,n_T-1} & \overline{h}^*_{k,n_T} & \tilde{y}_{k,1} & \tilde{y}_{k,2} \\ \overline{h}_{k+1,k} & \overline{h}^*_{k+1,k+1} & \cdots & \overline{h}_{k+1,n_T-1} & \overline{h}^*_{k+1,n_T} & \tilde{y}_{k+1,1} & \tilde{y}_{k+1,2} \\ \vdots & \vdots & \ddots & \vdots & \vdots & \vdots & \vdots \\ \overline{h}_{n_R,k} & \overline{h}^*_{n_R,k+1} & \cdots & \overline{h}_{n_R,n_T-1} & \overline{h}^*_{n_R,n_T} & \tilde{y}_{n_R,1} & \tilde{y}_{n_R,2} \end{bmatrix}. \tag{28}$$

Once the matrix H^{ala}_{div} is built, the next step is to apply the Sorted QR decomposition on it. This calculation may be carried out using Algorithm 2 below. The matrices R^{div} and $\tilde{Y}^{div}$ generated in this part of the process represent the contribution of diversity layers in the *HC Sorted QR* decomposition. The matrices R_{LD} and $\tilde{Y}_{LD}$ are generated from the matrices R^{spa}, R^{div}, $\tilde{Y}^{spa}$ and $\tilde{Y}^{div}$. The construction process is described in Algorithm 3. Once the matrices R_{LD} and $\tilde{Y}_{LD}$ are generated the detection of the received symbols is carried out according to the procedure described in section IV-B.

V. Results

In this section we compare the performance of VBLAST, DSTTD and the Hybrid code. In all cases, we consider four antennas in the transmitter and four in the receiver. Also, the modulation used in each case has been adjusted so that 12 bits are transmitted per channel use, as described in Table II above.

In Figure 9 we compare the bit error rate (BER) of the three codes. It can be observed that the Hybrid code proposed here outperforms the other two codes. It is also important to note that VBLAST's BER vs SNR curve has constant slope for high SNR. This means that VBLAST has no ability to exploit channel diversity. This is consistent with its spatial-multiplexing nature. The other two codes, by repeating data over different time and space channels, do take advantage of the channel's diversity.

In Figure 10, we compare the BER performance of the Hybrid code when the receiver's QR decomposition is implemented using the Modified Gram-Schmidt algorithm, and also when it is implemented using CORDIC. It can be seen that seven CORDIC iterations are enough to achieve the same

Algorithm 2 Diversity Decomposition of *HC Sorted QR* using Givens Rotations

```
INPUT: H^{ala}_{div}, n_S, n_B, L, order.
OUTPUT: R^{div}, Ỹ^{div} and order
R^{div} = H^{ala}_{div}, m = L n_S ,index = 1.
for i = 1 : i = i + 2 to 2n_B do
    k = argmin_{j=i:2:2n_B} ||R^{div}(:, j)||_2
    Exchange columns k and k + 1 for i and i + 1 of R^{div}.
    Exchange columns m + Li and m + Li − 1 for m + Lk and
m + Lk − 1 of vector order
    for l = index to n_R do
        [x_1 θ_1]=V(Re(R^{div}(l,i)),Im(R^{div}(l,i)))
        [x_2 θ_2]=V(Re(R^{div}(l,i+1)),Im(R^{div}(l,i+1)))
        R^{div}(l,i)=x_1+j*0,    R^{div}(l,i+1)=x_2+j*0
        theta1(l)=−θ_1,    theta2(l)=−θ_2
        for m = i + 2 : 2 to n_T + L do
            [x_r x_i]=R(Re(R^{div}(l,m)),Im(R^{div}(l,m)),θ_1)
            R^{div}(l,m)=x_r+j*x_i
        end for
        for m = i + 3 : 2 to n_T + L do
            [x_r x_i]=R(Re(R^{div}(l,m)),Im(R^{div}(l,m)),θ_2)
            R^{div}(l,m)=x_r+j*x_i
        end for
    end for
    for l = index to n_R do
        [x_r φ]=V(Re(R^{div}(l,i)),Re(R^{div}(l,i+1)))
        R^{div}(l,i)=x_r+j*0,    R^{div}(l,i+1)=0+j*0
        for m = i + 2 : 2 to n_T + L do
            [x_{r1} x_{r2}]=R(Re(R^{div}(l,m)),Re(R^{div}(l,m+1)),φ)
            [x_{i1} x_{i2}]=R(Im(R^{div}(l,m)),Im(R^{div}(l,m+1)),φ)
            R^{div}(l,m)=x_{r1}+j*x_{i1} ,    R^{div}(l,m+1)=x_{r2}+j*x_{i2}
        end for
    end for
    for l = index to n_R do
        for m = i + 3 : 2 to n_T + L do
            [x_{r1} x_{i1}]=R(Re(R^{div}(l,m)),Im(R^{div}(l,m)),theta_1(l))
            [x_{r2} x_{i2}]=R(Re(R^{div}(l,m)),Im(R^{div}(l,m)),theta_2(l))
            R^{div}(l,m)=x_{r1}+j*x_{i1} ,    R^{div}(l,m)=x_{r2}+j*x_{i2}
        end for
    end for
    for l = index : −1 to index + 1 do
        [x_r φ]=V(Re(R^{div}(l−1,i)),Re(R^{div}(l,i)))
        R^{div}(l−1,i)=x_r+j*0,    R^{div}(l,i)=0+j*0
        for m = i + 2 to n_T + L do
            [x_{r1} x_{r2}]=R(Re(R^{div}(l−1,m)),Re(R^{div}(l,m)),φ)
            [x_{i1} x_{i2}]=R(Im(R^{div}(l−1,m)),Im(R^{div}(l,m)),φ)
            R^{div}(l−1,m)=x_{r1}+j*x_{i1},    R^{div}(l,m)=x_{r2}+j*x_{i2}
        end for
    end for
    index = index + 1
end for
Ỹ^{div}= [ R^{div}(1,n_T+1)      R^{div}(1,n_T+2)
                 ⋮                      ⋮
           R^{div}(n_B,n_T+1)    R^{div}(n_B,n_T+2) ]
```

Algorithm 3 Procedure to obtain R_{LD} and $\tilde{Y}_{LD}$ from R^{spa}, R^{div}, $\tilde{Y}^{spa}$ and $\tilde{Y}^{div}$

INPUT: R^{spa}, R^{div}, $\tilde{Y}^{spa}$, $\tilde{Y}^{div}$, n_S, n_B.
OUTPUT: R_{LD}, $\tilde{Y}_{LD}$.
Let $R_{LD}^{2n_R \times 2(n_S+nB)} = 0$.
Build R_{LD}^{spa} and R_{LD}^{A}
$row{=}1$
for $k = 1$ to n_S **do**
  $R_{LD}^{spa}(row,1{:}2{:}2n_S{-}1){=}R^{spa}(k,1{:}n_S)$
  $R_{LD}^{spa}(row{+}1,2{:}2{:}2n_S){=}{-}R^{spa}(k,1{:}n_S)^*$
  $row{=}row{+}2$
end for
$row{=}1,\ col{=}2n_S{+}1$
for $i = 1$ to $n_S + n_B$ **do**
  for $j = 1$ to n_B **do**
    $R_{LD}^{spa}(row,col){=}R^{spa}(i,2j{-}1{+}n_S)$
    $R_{LD}^{spa}(row,col{+}1){=}R^{spa}(i,2j{+}n_S)$
    $R_{LD}^{spa}(row{+}1,col){=}R^{spa}(i,2j{+}n_S)^*$
    $R_{LD}^{spa}(row{+}1,col{+}1){=}{-}R^{spa}(i,2j{-}1{+}n_S)^*$
    $col{=}col{+}2$
  end for
  $col{=}2n_S{+}1$
  $row{=}row{+}2$
end for
$R_{LD}^{A}(2{*}n_S{+}1{:}2{*}(n_S{+}n_B),2{*}n_S{+}1{:}2{*}(n_S{+}n_B)){=}R^{div}$
$R_{LD}{=}\begin{bmatrix} R_{LD}^{spa} \\ R_{LD}^{A} \end{bmatrix}$,
Build vector $\tilde{Y}_{LD}$
$rows{=}1$
for $k = 1$ to n_S **do**
  $\tilde{Y}_{LD}^{spa}(rows,1){=}\tilde{Y}^{spa}(k,1)$
  $\tilde{Y}_{LD}^{spa}(rows{+}1,1){=}\tilde{Y}^{spa}(k,2)$
  $rows{=}rows{+}2$
end for
$rows{=}1$
for $k = 1$ to $2n_B$ **do**
  $\tilde{Y}_{LD}^{div}(rows,1){=}\tilde{Y}^{div}(k,1)$
  $\tilde{Y}_{LD}^{div}(rows{+}1,1){=}\tilde{Y}^{div}(k,2)$
  $rows{=}rows{+}2$
end for
$\tilde{Y}_{LD}{=}\begin{bmatrix} \tilde{Y}_{LD}^{spa} \\ \tilde{Y}_{LD}^{div} \end{bmatrix}$

performance. The relevance of this result is that it is essential when implementing the receiver in digital hardware.

Finally, we present the effect of correlation on the performance of the Hybrid code. In Figure 11, we show that there is a severe loss (around 5dB) of performance in the case of Laplacian correlation, compared to the uncorrelated channel. This is to be expected, since channel correlation means that symbols transmitted at different times and over different antennas are, however, still subject to similar conditions. This has the effect of reducing the code's diversity gain. Note, however, that CORDIC is still able to match the performance of the MGS algorithm. In some cases (for instance, VBLAST), the number of iterations required increases when correlation is present.

VI. Conclusions

We have presented the theory behind space-time codes and their potential for increasing data rate and reliability in

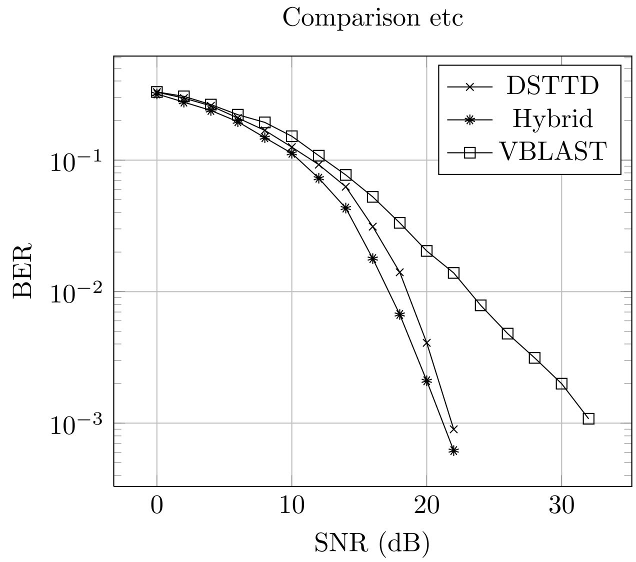

Fig. 9: Bit-error rate comparison between DSTTD, hybrid, and V-BLAST space-time codes. The hybrid code described here is the better performer.

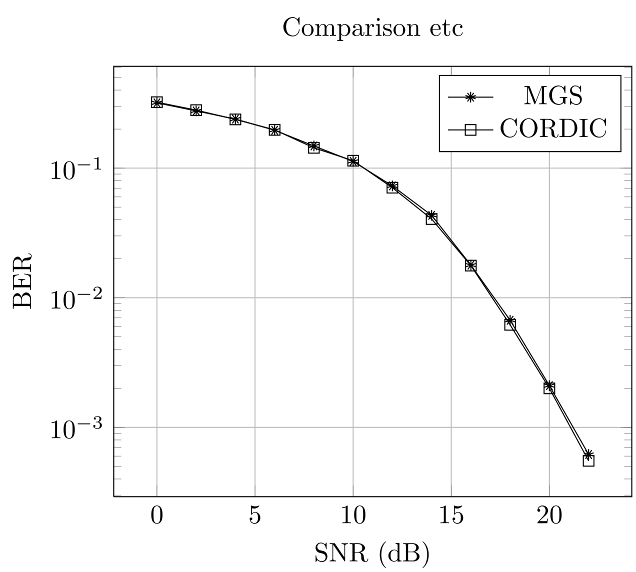

Fig. 10: A comparison between code performance when the QR decomposition in the receiver is performed using the modified Gram-Schmidt algorith or with CORDIC. Here, the CORDIC performs seven rotations, which are enough to reach the best peformance.

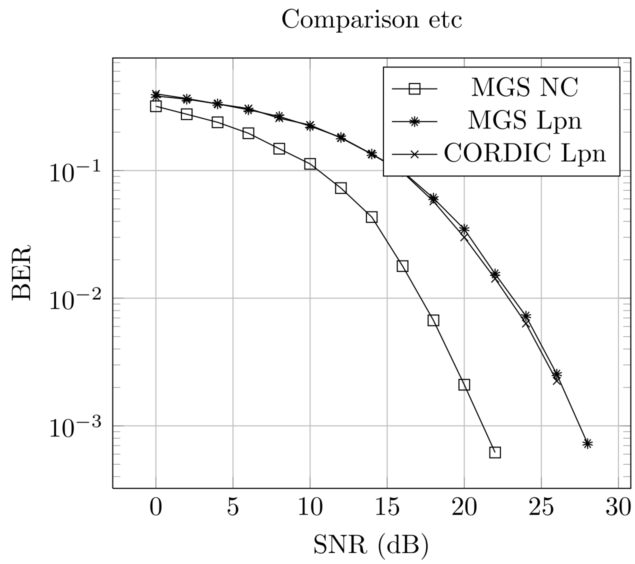

Fig. 11: Hybrid code performance loss when the channel presents Laplacian correlation. Under this channel, the CORDIC requires 8 iterations to reach the performance predicted by the modified Gram-Schmidt algorithm.

wireless systems. We have presented a hybrid code that uses V-BLAST and Alamouti codes at the same time and presents better performance than both of them, at the same data rate. We have also shown that channel correlation may significantly reduce the performance of these codes, and it remains a challenge in their practical operation.

The close relationship between hybrid space-time codes and linear dispersion codes has been established. The proposed approach has several advantages: from the point of view of linear dispersion codes a new way to design codes significantly easier than the original approach in [8] has been introduced. From the perspective of hybrid systems, a performance enhancement can be obtained without increasing the decoder's complexity neither sacrificing the spectral efficiency. The ZF LD STBC-VBLAST architecture is a reformulation of the hybrid system equation that permits to implement a decoding scheme equivalent to another purely spatial. The particular arrangement of the H_{LD} matrix elements does not increase the numerical complexity on the *HC Sorted QR* algorithm.

References

[1] I. E. Telatar, "Capacity of multiple-antenna Gaussian channels", *European Transactions on Telecommunications*, vol. 10, no. 6, pp. 585-595, 1999.

[2] Gesbert, D.; Bolcskei, H.; Gore, D.A.; Paulraj, .J, "Outdoor MIMO wireless channels: models and performance prediction." *IEEE Transactions on Communications*, vol. 50, no. 12, Dec. 2002, pp. 1926-1934.

[3] R. Parra-Michel, A. Alcocer-Ochoa, A. Sanchez-Hernandez, and Valeri Kontorovich. "Recent Advances in Signal Processing". Chapter "MIMO Channel Modeling and Simulation". ISBN 978-953-7619-41-1. I-Tech Education and Publishing KG.

[4] D–S Shiu, G. J. Foshini, M. J. Gans & J. M. Kahn, "Fading Correlation and Its Effect on the Capacity of Multielement Antenna systems," *IEEE Transactions on Communications*, Vol. 48, No. 3, pp 502-512, March 2000.

[5] G. J. Foschini, "Layered space-time architecture for wireless communication in a fading environment when using multi- element antennas," *Bell Laboratory Technology Journal*, Vol. 1, No. 2, pp 41-51, 1996.

[6] N. Seshadri V. Tarokh, A. Naguib and A. R. Calderbank, "Combined array processing and space-time coding," *IEEE Transactions on Information Theory*, Vol. 45, No. 4, pp 1121-1128, 1999.

[7] L. Zheng and D. Tse, "Diversity and multiplexing: fundamental tradeoff in multiple antenna channels", *IEEE Transactions on Information Theory*, vol. 49, pp. 1073-96, May 2003.

[8] B. Hassibi and B. M. Hochwald, "High-rate codes that are linear in space and time," *IEEE Transactions on Information Theory*, vol. 48, pp. 1804-1824, 2002.

[9] J. Cortez et al, "An efficient detector for non-orthogonal Space-Time Block Codes with Receiver Antenna Selection," in *Proc. of* 18^{th} *Int. Symp. on Personal, Indoor and Mobile Radio Communications*, September 2007, Greece.

[10] J. Cortez et al, "Generalized ABBA-V-BLAST Hybrid Space-Time Code for Wireless Communications," in *Proc. of* 9^{th} *IEEE International Workshop on Signal Processing Advances in Wireless Communications (SPAWC 2008)*, August 2008, Brazil.

[11] X. Nam TRAN et al, "Performance Comparison of Detection Methods for Combined STBC and SM Systems", *IEICE Transaction on Communications*, vol. E91-B, No. 6 pp. 1734-1742,2008.

[12] T. Mao and M. Motani, "STBC-VBLAST for MIMO wireless communication systems," in *Proc. of Int. Conf. on Communications*, vol. 4, pp. 2266-2270, May 2005.

[13] L. Zhao and V. K. Dubey, "Detection Schemes for Space-time Block Code and Spatial Multiplexing Combined System," *IEEE Communication Letters*, vol. 9, no. 1, January 2005.

[14] O. Longoria-Gandara et al, "Linear Dispersion Codes Generation from Hybrid STBC-VBLAST Architectures," in *Proc. of* 4^{th} *Int. Conf. on Electrical and Electronics Engineering*, 2007.

[15] S. M. Alamouti, "A simple transmit diversity technique for wireless communications", *IEEE Journal on Selected Areas in Communications*, vol. 16, no. 8, October 1998, pp. 1451-1458.

[16] D. Wubben et al, "Efficient algorithm for decoding layered space-time codes", *Electronics Letters*, vol. 37, pp. 1348-150, 2001

[17] P. Luethi et al, "VLSI Implementation of High-Speed Iterative Sorted MMSE QR Decomposition," in *Proc. of IEEE International Symposium on Circuits and Systems*, pp. 1421-1424, 2007.

[18] Ray Andraka, "A survey of CORDIC algorithms for FPGA based computers," in *Proc. of the ACM/SIGDA sixth international symposium on Field programmable gate arrays*, vol. 4, pp. 191-200, 1998.